DOI: 10.61782/fa.2023.0638

forum acusticum 2023

ACOUSTIC PROPERTIES STUDY OF ANISOTROPIC POROUS MATERIALS THROUGH THE BIOT MODEL APPLIED WITH A FINITE ELEMENT MODEL

María Mónica Ballesteros Villarreal[1,2*] **Jonas Brunskog**[1] **Mads Bolberg**[2]
[1] Acoustic Technology Group, Technical University of Denmark, Denmark
[2] ROCKWOOL A/S, Denmark

ABSTRACT

The available information about the acoustic properties of current building industry materials, specifically porous materials, is scarce, and the models that describe their properties are mostly empirical or oversimplified, e.g., the equivalent fluid models. This study works with a glass wool sample, described through the Biot model, which explains the interaction between the fluid and the porous matrix in more detail, where the equivalent density and bulk modulus of the material are obtained through the Johnson-Champoux-Allard model. The models consider the anisotropy of the airflow resistivity and elastic parameters of the porous material, and they are followed by a sensitivity study. The models are implemented through a finite element modeling tool, and the results of the study show the most important parameters in this specific situation. The final model may provide a more general tool for optimizing the materials.

Keywords: *Fibrous materials, orthotropy, finite element modelling, airflow resistivity.*

1. INTRODUCTION

Porous materials are important in the building industry when it comes to heat insulation, sound absorption and sound insulation. The acoustic behavior of these materials is understood to a certain extent due to the models that have been developed. The simplest of these are the empirical equivalent fluid models [1, 2]. Through time, a diphasic model developed by Biot [3, 4], and semi-phenomenological models [5–8] have been developed to describe the wave propagation in porous materials more accurately. The capacity of the models depends directly on the parameters that can be characterized from these materials: the more parameters the model has, the more details of the behavior of the material can be explained. More complex models can show specific acoustic behaviors not seen with simpler models, and these behaviors can be exploited when understood. However, the more advanced models require parameters that are not commonly available or easy to characterize.

Strictly speaking, porous materials used for sound absorption and sound insulation are anisotropic and inhomogeneous due to the manufacturing process [9]. For many applications, it is safe to assume that the porous materials are isotropic and homogeneous, and the predictions will have good enough correspondence to measured results. However in some important situations, this is not the case. Moreover, including the anisotropic nature of porous materials can give more room for product development and optimization. In the case of melamine foam, it is a material generally assumed isotropic even though the small effects of its anisotropy can be measured as in [10]. Glass wool is known to be transversely isotropic, and considering this in a model, can lead to results which show the actual differences in the acoustic performance depending on the incidence angle [11, 12]. Stone wool fibers' anisotropy is not quite as in glass wool [13], the material's fibers differ in diameter distribution, anisotropy parameter, and other aspects, and this can be of importance in the sound performance.

**Corresponding author*: *mmbv@dtu.dk.*

As aforementioned, anisotropic parameters can be difficult to characterize experimentally, leading to scarce available information about the parameters. If we want to use the more complex models, we have to combine sources and/or estimate the missing parameters. This is yielding uncertainty and perhaps inaccurate results [14].

This work is preliminary research of a project which aims to describe the wave propagation in porous materials through a reliable finite element model based on the Biot theory [3, 4]. It takes into account anisotropic parameters, more specifically the airflow resistivity and the poroelastic parameters, while still assuming that the materials are homogeneous. The intention is to develop one single model in finite element modeling that contemplates the anisotropy in all the aforementioned parameters, which is currently not available or easily found. This paper applies a version of the Johnson-Champoux-Allard (JCA) model with a transversely isotropic airflow resistivity, and the Biot model with transversely isotropic elastic parameters [6, 11]. Now a combined implementation of both anisotropic airflow and elastic parameters is starting to be investigated. By comparing the effect of anisotropic airflow in JCA and anisotropic elastic properties we try to investigate if both aspects are important, and in what way.

The aim of this paper is to assess the impact of the anisotropy of these parameters, using information from a glass wool sample [15]. The consequence of it is building a strong base that helps put together both models and allow to include the anisotropy of any parameters needed in further investigations.

This paper is organized as follows. The first section gives an introduction to the relevant theory of the equivalent fluid model from Johnson-Champoux-Allard (JCA) [5–7], as well as the Biot theory [3, 4, 16], the anisotropic versions of both models, and the connection between these two models. The following sections include the preliminary results of the models applied to a glass wool sample, along with a sensitivity study and a discussion about these results.

2. THEORY AND METHOD

2.1 Theory

A semi phenomenological equivalent fluid model, the Johnson-Champoux-Allard (JCA) [5,6,11,15] model, and a diphasic model, the Biot-Allard [4, 6] model (denoted Biot hereafter) are used for describing the wave propagation. The JCA model yields an equivalent density ρ_{eq} and equivalent bulk modulus K. The Biot model yields the characteristic impedance Z_c and the complex wavenumber k. These four properties (ρ_{eq}, K, Z_c, k) can be used to calculate the sound absorption coefficients α.

2.1.1 The JCA model with orthotropic airflow resistivity

The JCA model [5, 6, 11, 15] is an equivalent fluid model, which considers the frame or skeleton as motionless and only models the motion in the fluid phase. It is used to describe the visco thermal dissipative effects through five parameters from the porous material: porosity ϕ, specific airflow resistivity r, tortuosity α_∞, viscous characteristic length Λ, and thermal characteristic length Λ'. As pointed out in [6], anisotropic porous media's parameters which describe the viscous inertial interactions between both phases can be considered as diagonal tensors in three orthogonal directions. In the case of glass wool, the model can consider a specific scenario of anisotropy such as transversely isotropic (TI) properties. As Nennig indicates [6, 15], the equivalent bulk modulus in the JCA model of a TI fluid, will not be affected by anisotropy, therefore yields

$$K_{eq} = \frac{\gamma P_0/\phi}{\gamma-(\gamma-1)\left[1-j\frac{8\kappa}{\Lambda'^2 C_p \rho_0 \omega}\sqrt{1+j\frac{\Lambda'^2 C_p \rho_0 \omega}{16\kappa}}\right]^{-1}} \tag{1}$$

where γ refers to the ratio of specific heats, κ is the thermal conductivity, ρ_0 the density of air and C_p the specific heat at constant pressure. It is also mentioned that air flow resistivity can be represented as a second-order diagonal tensor, $\mathbf{r} = \mathrm{diag\,r^k}$ where $k = T, I, I$ are transverse and isotropic directions, according to Nennig which treats the specific case of a TI material. In a general case, the directions can be assumed as the x, y, and z axis. Thus in this paper the equivalent density is assumed to be dependent on the orthotropic airflow resistivity $\mathbf{r} = (r_x, r_y, r_z)$, resulting in the tensor

$$\rho_{eq} = \begin{pmatrix} \rho_x & 0 & 0 \\ 0 & \rho_y & 0 \\ 0 & 0 & \rho_z \end{pmatrix}, \tag{2}$$

where each density value is

$$\rho_x = \frac{\rho_0 \alpha_\infty}{\phi}\left[1+\frac{r_x \phi}{j\omega\rho_0\alpha_\infty}\sqrt{1+j\frac{4\alpha_\infty^2 \eta \rho_0 \omega}{r_x^2 \Lambda^2 \phi^2}}\right], \tag{3}$$

where η is the dynamic viscosity, and the densities ρ_y, ρ_z will have a corresponding form.

2.1.2 The Biot model with transversely isotropic elastic parameters

The Biot model [3, 4, 16] considers the interaction between a solid and a fluid phase, e.g. the mineral wool and the air, respectively. The theory assumes that there is a coupling between the two phases, unlike the previous model which assumes that the solid phase is motionless. Biot [16] uses Darcy's law to represent the anisotropic permeability properties of the material when defining the field equations for the distribution of stress and deformation of a porous viscoelastic anisotropic solid. Darcy's law is included in Biot's model through a symmetric matrix to which he refers to as the *flow resistance matrix*. This matrix, along with the stress components and the equilibrium equations defined, are used to define the displacements between the fluid and porous phases. In this specific case, the anisotropy of the airflow resistivity would be considered as part of the equivalent density that was obtained in the JCA model. In this paper, the anisotropic airflow resistivity will only be considered in the JCA model, and the anisotropic elastic parameters will be considered only in the Biot model. Both types of anisotropy (airflow resistivity and elastic parameters) are not included in the Biot model in most of the literature that makes use of the model.

The finite element model software used is COMSOL Multiphysics [17], where the theory for implementing the Biot model is developed as follows: The poroelastic wave equations as expressed by Biot are

$$\begin{aligned} -\rho_{av}\omega^2\mathbf{u} + \rho_f\omega^2\mathbf{w} - \nabla\cdot\sigma &= 0 \\ -\rho_f\omega^2\mathbf{u} - \omega^2\rho_c(\omega)\mathbf{w} + \nabla p_f &= 0 \\ \rho_c(\omega) = \frac{\alpha_\infty}{\phi}\rho_f + \frac{\mu_f}{i\omega\kappa} & \end{aligned} \tag{4}$$

where **u, w** are the displacement of the solid and fluid phase, respectively. The average density is the combined density of the solid and fluid phases together expressed as $\rho_{av} = \rho_d + \phi\rho_f$, where p_f is the fluid pore pressure and ϕ is the porosity. The complex density ρ_c is formed by the ρ_f and μ_f which are the density and viscosity of the fluid, α_∞ is the tortuosity, and κ the permeability. The total stress tensor of the solid phase is σ. This stress tensor in a transversely isotropic analysis, along with strain components e_{ij} result in relations where the elastic parameters can be found [6]. The strain components are $e_{ij} = 1/2(\delta u_i^s/\delta x_j + \delta u_j^s/\delta x_i)$ when considering the X-axis to be the normal axis, the stress-strain relations for the frame in vacuum are

$$\begin{aligned} \hat{\sigma}_{xx} &= Fe_{zz} + Fe_{yy} + Ce_{xx} \\ \hat{\sigma}_{yy} &= Ae_{zz} + (2G + A)e_{yy} + Fe_{xx} \\ \hat{\sigma}_{zz} &= (2G + A)e_{zz} + Ae_{yy} + Fe_{xx} \\ \hat{\sigma}_{yx} &= 2G'e_{yx} \\ \hat{\sigma}_{xz} &= 2G'e_{xz} \\ \hat{\sigma}_{zy} &= 2Ge_{zy}, \end{aligned} \tag{5}$$

where A, F, G, C, and G' are the rigidity coefficients. If the Young's modulus is considered transversely isotropic as it is in this paper, then the Young's modulus is expressed as $E_y = E_z = E$ and $E_x = E'$, with the Poisson ratios being $\nu_{yz} = \nu, \nu_{xy} = \nu_{xz} = \nu'$, therefore the relation between the rigidity coefficients and the elastic coefficients is

$$\begin{aligned} A &= \frac{E(E'\nu + E\nu'^2)}{(1+\nu)(E' - E'\nu - 2E\nu'^2)} \\ F &= \frac{EE'\nu'}{E' - E'\nu - eE\nu'^2} \\ C &= \frac{E'^2(1-\nu)}{E' - E'\nu - 2E\nu'^2} \\ G &= \frac{E}{2(1+\nu)}. \end{aligned} \tag{6}$$

According to COMSOL, the formulation for the displacements **u, w** is not convenient from the numerical point of view, so the approach for the Biot model is through solving for the fluid pore pressure variable p_f instead of the fluid displacement **w**, since pressure is a scalar and displacement is a vector, the **u**-p formulation would mean having fewer degrees of freedom. The wave equations in (4) become

$$\begin{aligned} -\rho_{av}\omega^2\mathbf{u} - \frac{\rho_f}{\rho_c(\omega)}(\nabla p_f - \rho_f\omega^2\mathbf{u}) - \nabla\cdot\sigma &= 0 \\ \mathbf{w} = \frac{1}{\omega^2\rho_c(\omega)}(\nabla p_f - \rho_f\omega^2\mathbf{u}). & \end{aligned} \tag{7}$$

If the terms are arranged in terms of the variables **u** and p for the first row and we take the divergence for the second row

$$\begin{aligned} -(\rho_{av} - \frac{\rho_f^2}{\rho_c(\omega)}\omega^2\mathbf{u} - \nabla\cdot(\sigma_d(\mathbf{u}) - \alpha_B p_f\mathbf{I}) &= \frac{\rho_f}{\rho_c(\omega)}\nabla p_f \\ \omega^2\nabla\cdot(\frac{\rho_f}{\rho_c(\omega)}\mathbf{u}) + \omega^2\nabla\cdot\mathbf{w} + \nabla\cdot(-\frac{1}{\rho_c(\omega)}\nabla p_f) &= 0, \end{aligned} \tag{8}$$

by using the expression from the volumetric strain $\varepsilon_{vol} = \nabla \cdot \mathbf{u}$ and fluid displacement

$$-\nabla \cdot \mathbf{w} = \frac{p_f}{M} + \alpha_B \varepsilon_{vol}, \tag{9}$$

where Biot's modulus M is calculated from the porosity ϕ, fluid compressibility χ_f, Biot-Willis coefficient α_B and the drained bulk modulus of the porous matrix K_x as

$$\frac{1}{M} = \phi\chi_f + \frac{\alpha_b - \phi}{K_d}(1 - \alpha_B). \tag{10}$$

But when both thermal and viscous losses are included, as it is in this case, the viscosity in the complex density seen in Eq. (4) and the compressibility from Eq. (10) are frequency dependent. The losses due to viscosity are considered by the viscosity expression and the losses due to thermal conduction by the fluid compressibility expression [6].

The frequency dependent complex viscosity is given by

$$\mu(\omega) = \mu\sqrt{(1 + \frac{4i\omega\alpha_\infty^2\mu\rho_f}{r^2\Lambda^2\phi^2}}), \tag{11}$$

and the frequency-dependent complex fluid compressibility is given by

$$\chi_f(\omega) = \frac{1}{\gamma p_a}\left[\frac{\gamma - (\gamma - 1)}{(1 + \frac{8\mu}{i\omega\Lambda'^2 Pr\rho_f}\sqrt{1 + \frac{i\omega\Lambda^2 Pr\rho_f}{16\mu}}}\right], \tag{12}$$

where $Pr = \Lambda/\Lambda'$ is the Prandtl number. These two expressions are used in the JCA model to find the bulk modulus and equivalent density as in Eq. 1 and Eq. 3.

Then, in Eq. 8, the bottom row, simplifies to

$$\omega^2\nabla \cdot \left(\frac{\rho_f}{\rho_c(\omega)}u\right) - \omega^2\left(\frac{1}{M}\rho_f + \alpha_B\varepsilon_v ol\right) + \nabla \cdot \left(-\frac{1}{\rho_c(\omega)}\right)\nabla p_f = 0 \tag{13}$$

and finally, Biot's wave equations, first row of Eq. 8, and Eq. 13 can be written in terms of the variable $\mathbf{u}$ and p_f as:

$$\begin{aligned} -\omega^2\left(\rho_{av} - \frac{\rho_f^2}{\rho_c(\omega)}\right)\mathbf{u} - \nabla \cdot (\sigma_d(\mathbf{u}) - \alpha_B p_f \mathbf{I}) &= \frac{\rho_f}{\rho_c(\omega)}\nabla p_f \\ -\frac{\omega^2}{M}p_f + \nabla \cdot -\frac{1}{\rho_c(\omega)}(\nabla p_f - \omega^2\rho_f\mathbf{u}) &= \omega^2\alpha_B\varepsilon_{vol} \end{aligned} \tag{14}$$

2.2 Method

2.2.1 Data compilation

The material considered is glass wool, the data used for the simulations has been obtained from Nennig et. al [15]. The data is presented in Table 1. Nennig et. al worked on a transverse isotropic equivalent fluid model that combines limp and rigid frame behaviors, choosing the rigid or limp approach depending on the propagation direction, e.g. limp approach for the transverse direction and rigid for the normal direction. All the material parameters needed for the models in this paper are characterized and reported in their work. They report transversal isotropy data for r, Λ, and E, therefore this information can be used in both the JCA and Biot anisotropic models.

Table 1. Table of parameters with the information from [15]. * Poisson's ratio is assumed to be zero for fibrous materials as in [18].

Source	**Nennig**		
Material	Glass wool		
Parameter			
h [mm]	50.8	E or E_x [Pa]	670
ϕ	0.98	E_y [Pa]	142000
α_∞	1.0	E_z [Pa]	142000
Λ [μm]	295	ν or ν_x	0*
Λ' [μm]	708	ν_y	0*
ρ [kg m^{-3}]	16	ν_z	0*
η	0.1	G or G_x [MPa]	3520
r or r_x [Pa s m^{-2}]	38000	G_y [MPa]	3520
r_y [Pa s m^{-2}]	16720	G_z [MPa]	3520
r_z [Pa s m^{-2}]	16720		

2.2.2 Implementation in COMSOL

An impedance tube scenario was modelled by having a cylindrical geometry of 0.10 m diameter and 0.30 m length of air with sound hard boundaries, simulating the impedance tube and referred to as the air domain, where the pressure acoustics COMSOL node was used. The porous domain would have the same diameter and also sound hard boundaries, considering the back end of the tube and no air gap after the porous domain. For the JCA model, the anisotropic acoustics node is used. In this node the equivalent density and bulk modulus has to be input directly, therefore the values are the formulas for bulk modulus and equivalent density that depend on frequency, as in Eqs. 1 and 3. For the density, a symmetric

matrix is chosen and filled out with the formulas including the appropriate direction of the airflow resistance. The absorption coefficient is calculated by comparing the incident and outgoing power at the "entrance" of the tube as $\alpha = 1 - (P_{out}/P_{in})$. The Biot model in COMSOL was implemented by using the poroelastic waves node on the porous domain. The Biot model with thermal and viscous losses was selected as well as a drained matrix, orthotropic configuration, which allows to input the elasticity parameters in 3x3 matrices. Regarding the boundary conditions, two scenarios were simulated. First a sample clamped to the tube walls, to include the resonance effects that can be observed in impedance tube measurements under such mounting conditions [19]. The second scenario includes a sample with periodic boundary conditions which simulates an infinitely large sample is done using Floquet periodicity, although the effects of the clamped sample cannot be seen here, this configuration allows to study different angles of incidence in the sample, to understand better the effect of anisotropy of the material. The absorption coefficient is calculated as in JCA by comparing the input and output power in the system.

2.2.3 *Sensitivity and parameter study*

A sensitivity study was carried out to understand the impact that the change in a parameter will have in the absorption coefficient.This shows to what parameters is the system more prone to change and leads to conclusions around which parameters' data can be assumed safely and which ones have to be carefully characterized [14, 20]. The sensitivity study assumes that the material is isotropic and under normal incidence conditions.

3. RESULT AND ANALYSIS

The results for the simulations can be seen in Fig. 1, where the comparison between models is done as well as the boundary conditions and anisotropy conditions. These are at the same time compared to the measured results reported in Nennig's paper [15]. At a first glance, it is interesting to see that the JCA models results, both the infinite isotropic and anisotropic, are perfectly overlapped. This is due to the incidence angle being normal, so the anisotropy of the airflow resistivity is neglected. The airflow resistivity of the other directions was modified considerably and the results remained the same. The difference of the JCA models from the measured results and the Biot models is noticeable. The high absorption coefficient seen in the frequencies prior to 1 kHz for the Biot model and the measurements is due to the effects of the skeleton or solid phase that is neglected by the JCA model. Therefore the contribution of the JCA model in the Biot model would be important when considering incidence angles or a more detailed anisotropy. Next, the Biot model results seen in this same figure include a clamped sample and the isotropic and anisotropic results. The isotropic results are smoother than the anisotropic, this is due to the effects of the elastic parameters as it can be seen the measured results adjust better to the anisotropic model. In the sensitivity study shown in Fig. 2, it can be seen that the parameters that are more important under the set conditions (isotropic and normal incidence) are the porosity, the thermal characteristic length, and the density. The airflow resistivity is not one of the most important, and when the analysis comparing the isotropy and anisotropy of the material under oblique incidence was carried out, the change in the values for the airflow resistivity did not change on the absorption coefficient results.

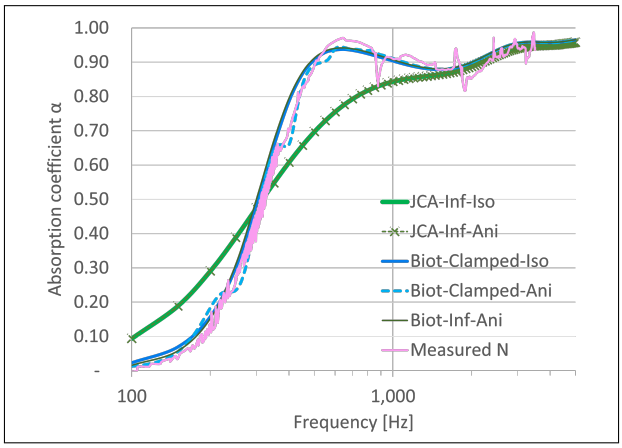

Figure 1. Sound absorption for different conditions of the glass wool comparing the two models JCA and Biot, the boundary conditions as clamped or infinite, and the isotropic and anisotropic conditions as well. The simulations are compared with the measured results reported by [15]

The results in Fig. 3 show the comparison of the models considering a normal incidence and a 60° incidence angle. This value was chosen from the results in Fig. 4, where the maximum absorption happens around 60° in both models. Fig. 3 shows first that the difference in the angle incidence for JCA shows only a higher absorption, but the behavior of the curve is almost the same, show-

Figure 2. Sensitivity analysis for the glass wool sample.

ing that the changes in the airflow resistivity due to the transversal anisotropy are not so important for this material. The material choice is important for this conclusions, since it has been seen in the parameter study used in previous work [14] that parameters may be much more sensitive between materials, such as stone wool. This invites to more research about the effects of the anisotropic airflow resistivity in stone wool. Next, the comparison between the anisotropy in the Biot model and the incidence angle as seen in Fig. 3 shows that the anisotropy not only shows small behaviors that are otherwise ignored, as the hip around 200 Hz. It also shows that if the incidence angle is changed, some effects like the dip seen around 2000 Hz might disappear and the absorption coefficient can increase almost to 1. The increase in absorption is greater in higher frequencies than in lower ones. The Biot model without clamping conditions (infinite sample), with anisotropic parameters and a normal incidence is the closest curve to the measurements. Nevertheless, since the measurements are also done inside an impedance tube, it would be of interest to have information about other measurements that can include changes in the incidence angle, as well as extending the model to calculate the results with random incidence. A simulation considering transversal incidence is added to the comparison, where it is clear that the behavior of the material is very different, especially around the frequencies from 300 Hz to 600 Hz, this effect is expected to be seen then under oblique incidence, especially grazing incidence. In Fig. 4 the absorption coefficient depending on the incidence angle can be seen, the study was done for several frequencies for isotropic and anisotropic conditions in an infinite sample. The top image which is done through the JCA model, shows that as previously said, the highest absorption comes after 60°, but it can be seen that for lower frequencies, the maximum absorption comes almost at grazing incidence. Since this is the JCA case, it means that the airflow resistivity in the y and z directions start to get more importance as long as the incidence is not normal, and that the lower frequencies will be the more influenced by this. This effect seems to be very similar if the material is isotropic or anisotropic. The effect of the oblique incidence seems to be very simi-

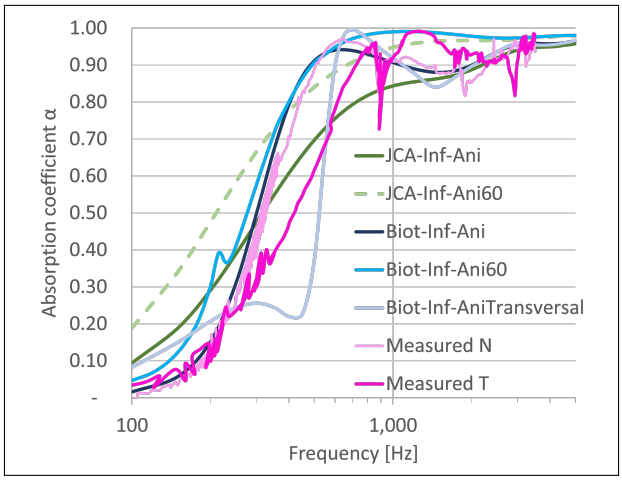

Figure 3. Sound absorption JCA model infinite sample in anisotropic conditions in normal incidence and oblique 60° incidence, Biot model infinite sample in anisotropic conditions in normal incidence and oblique 60° incidence, as well as transversal incidence, and compared to the two measurements provided by Nennig [15] impedance tube normal incidence measurements in the normal (N) and transversal (T) planes of the glass wool.

lar if the material is isotropic or anisotropic except on the lower frequencies for the JCA model. As for the bottom panel, the Biot model, it can be seen that the absorption increases when the incidence approaches grazing incidence, which is when the effects of the anisotropy are showing a bigger difference in Fig. 3.

4. DISCUSSION

The simulations of the JCA and Biot method for finite and infinite samples considering different anisotropic parameters for each model resulted in satisfactory first results for this project. The results showed that for this specific sample, in the JCA model, the effects of the anisotropy of the airflow resistivity are small and will only be seen through oblique incidence. This means that when comparing with measured data, it will be preferred to have

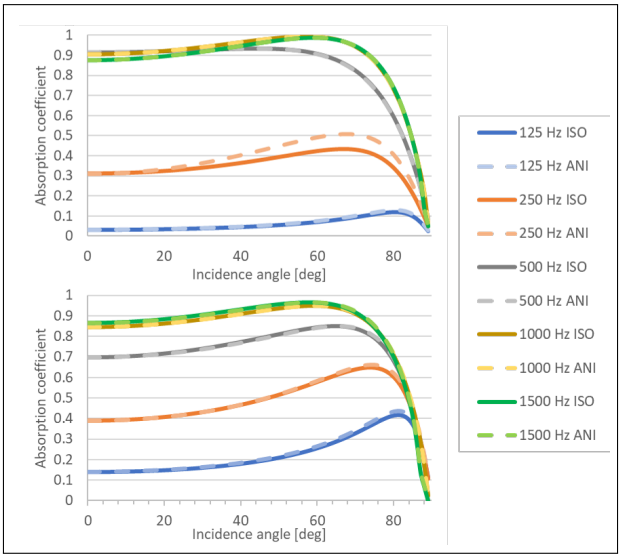

Figure 4. Angles of incidence vs. absorption coefficient for both the JCA model in isotropic and anisotropic conditions (top) and the Biot model in isotropic and anisotropic conditions (bottom).

results which include oblique incidence if we want to see anisotropic airflow resistivity effects. More information has to be gathered with respect to these results with other porous materials such as melamine foam or stone wool. The difference in absorption between the JCA and Biot model is considerable, as seen in Fig. 1. Considering the Biot model, under anisotropic conditions there are details in the results that are otherwise smoothed out when isotropy is assumed. In this Biot model case, the increase in the incidence angle show that the highest absorption for high frequencies happens around 60°, but this increase is not as notable as the one seen in the JCA model. The effects of the anisotropic parameters in both models have the same direction and are similar in size, which could mean that these effects add up when considered in one single model. The Biot model adjusts better to the presented measured results, but a full characterization which includes anisotropy can lead to a better model of the material, and this can help understand which are the most important parameters and how do they affect the acoustic behavior in the material. In many applications the use of the JCA model is enough, but as shown in Fig. 1, it can be clearly seen that for some specific details the Biot model can give more accurate results. Also reducing the measurements to an impedance tube can leave out information from the material that can be important, and measuring in a reverberant room may be difficult, methods like the one reported in [21] can provide a quick and accurate solution to the mentioned limitations. With a robust model, simulations can offer a better approach to get quick and accurate results, and complex scenarios can be simulated and studied better e.g. open plan offices, where a good decay is important and it depends on understanding what happens with the absorption under grazing incidence of the absorption panels of the place. Much more research considering other materials is needed to get proper robust conclusions, but for this to happen it is required to have materials fully characterized so the models are in order. An initial step is to join the JCA model to the Biot model in the software in COMSOL Multiphysics, so the equivalent density and bulk modulus which are the output of the JCA model, can be the input of the Biot model, all of this in one single model without having to work with them separately. It is important to state that this analysis is based on the results for one sample of glass wool. The sample analysed by [15] is an extreme case of mineral wool for sound absorption applications. Since its density and Young's modulus values differ a lot from actual absorbers used in the building industry environment, where the materials used have far higher stiffness and density values. This would potentially lead to a lower importance of the elastic parameters, since the case will be far closer to the rigid skeleton case in the equivalent fluid models, such as JCA.

5. CONCLUSIONS

The JCA and Biot models were used to simulate a sample of glass wool with anisotropic properties, different for each model. Clearly the Biot model shows the effects of both phases and therefore the results are more accurate to a real measurements than the JCA model, but they may complement each other well since one can hold information for the anisotropic airflow resistivity and the other for anisotropic elastic parameters. For this very specific material the incidence angle helps see better the effects of the anisotropic airflow resistivity and anisotropic elastic parameters, since the effects are very small. The behavior of glass wool may not be the same as in other porous materials so more research is needed, nevertheless it can be difficult since a good characterization of many parameters is needed for each material.

6. ACKNOWLEDGMENTS

The authors would like to acknowledge the Innovation Fund Denmark (grant case 1044-00182B). We also gratefully acknowledge Cheol-Ho Jeong (DTU) and Mads J. Herring Jensen (COMSOL) for their support and advise.

7. REFERENCES

[1] M. E. Delany and E. N. Bazley, "Acoustical properties of fibrous absorbent materials," *Applied Acoustics*, vol. 3, no. 2, pp. 105–116, 1970.

[2] Y. Miki, "Acoustical properties of porous materials – Modifications of Delany-Bazley models," *J. Acoust. Soc. Jpn*, vol. E, no. 11(1), pp. 19–24, 1990.

[3] M. Biot, "Theory of propagation of elastic waves in a fluid-saturated porous solid .1. Low-frequency range," *Journal of the Acoustical Society of America*, vol. 28, no. 2, pp. 168–178, 1956.

[4] M. Biot, "Theory of propagation of elastic waves in a fluid-saturated porous solid .2. High frequency range," *Journal of the Acoustical Society of America*, vol. 28, no. 2, pp. 179–191, 1956.

[5] D. Johnson, J. Koplik, and R. Dashen, "Theory of dynamic permeability and tortuosity in fluid-saturated porous-media," *Journal of Fluid Mechanics*, vol. 176, no. -1, pp. 379–402, 1987.

[6] J. F. Allard and N. Atalla, *Propagation of Sound in Porous Media: Modelling Sound Absorbing Materials*. John Wiley and Sons, 2009.

[7] Y. Champoux and J. Allard, "Dynamic tortuosity and bulk modulus in air-saturated porous-media," *Journal of Applied Physics*, vol. 70, no. 4, pp. 1975–1979, 1991.

[8] D. Lafarge, P. Lemarinier, J. F. Allard, and V. Tarnow, "Dynamic compressibility of air in porous structures at audible frequencies," *Acoustical Society of America. Journal*, vol. 102, no. 4, pp. 1995–2006, 1997.

[9] S. Schneider, "Experimental and numerical investigations on melamine wedges," *Journal of the Acoustical Society of America*, vol. 124, no. 3, pp. 1568–1576, 2008.

[10] C. Van Der Kelen and P. Göransson, "Identification of the full anisotropic flow resistivity tensor for multiple glass wool and melamine foam samples," *Journal of the Acoustical Society of America*, vol. 134, no. 6, pp. 4659–4669, 2013.

[11] P. Khurana, L. Boeckx, W. Lauriks, P. Leclaire, O. Dazel, and J. F. Allard, "A description of transversely isotropic sound absorbing porous materials by transfer matrices," *Journal of the Acoustical Society of America*, vol. 125, no. 2, pp. 915–921, 2009.

[12] V. Tarnow, "Measured anisotropic air flow resistivity and sound attenuation of glass wool," *Acoustical Society of America. Journal*, vol. Vol. 111, no. 6, pp. 2735–2739, 2002.

[13] L. Chapelle, "Characterization and modelling of the mechanical properties of mineral wool," 2016.

[14] M. M. Ballesteros Villarreal, J. Brunskog, and M. Bolberg, "Compilation of reference values in selected porous materials for sound propagation in finite element modelling," *Proceedings of Forum Acusticum*, vol. 2023-, 2023.

[15] B. Nennig, R. Binois, N. Dauchez, E. Perrey-Debain, and F. Foucart, "A transverse isotropic equivalent fluid model combining both limp and rigid frame behaviors for fibrous materials," *Journal of the Acoustical Society of America*, vol. 143, no. 4, pp. 2089–2098, 2018.

[16] M. Biot, "Theory of deformation of a porous viscoelastic anisotropic solid," *Journal of Applied Physics*, vol. 27, no. 5, pp. 459–467, 1956.

[17] COMSOL AB, "Comsol multiphysics®."

[18] H. J. Rice and P. Göransson, "A dynamical model of light fibrous materials," *International Journal of Mechanical Sciences*, vol. 41, no. 4-5, pp. 561–579, 1999.

[19] T. E. Vigran, L. Kelders, W. Lauriks, P. Leclaire, and T. F. Johansen, "Prediction and measurements of the influence of boundary conditions in a standing wave tube," *Acustica*, vol. 83, no. 3, pp. 419–423, 1997.

[20] M. Sadri, J. Brunskog, and D. Younesian, "Application of a bayesian algorithm for the statistical energy model updating of a railway coach," *Applied Acoustics*, vol. 112, pp. 84–107, 2016.

[21] M. Nolan, "Estimation of angle-dependent absorption coefficients from spatially distributed in situ measurements," *Journal of the Acoustical Society of America*, vol. 147, no. 2, pp. EL119–EL124, 2020.